Shahrood University of Technology

Journal of Mining and Environment (JME)

Journal homepage: www.jme.shahroodut.ac.ir

Iranian Society of Mining Engineering (IRSME)

Simultaneous Effects of Geometry, Lithology, Slope Angle, and Groundwater Level on the Slope Stability of Open Pit Mines (Case study of Golgohar Iron Ore Mine, Sirjan, Iran)

Mohammad Shekari Nejad[1], Mohammad Fatehi Marji[2*], and Manouchehr Sanei[2]

1. Department of Mining Engineering, si.c, Islamic Azad University, Sirjan, Iran
2. Department of Mining and Metallurgical Engineering, Yazd University, Yazd, Iran

Article Info

Received 4 March 2025
Received in Revised form 27 July 2025
Accepted 26 August 2025
Published online 26 August 2025

DOI: 10.22044/jme.2025.15867.3055

Keywords

Slope stability
Hydromechanical modelling
Drainage
Whole slope angle
Safety factor

Abstract

The slope geometry, rock mass quality, groundwater level, and geological features of the mine mainly influence the slope stability of an open-pit mine. In this study, the stability analysis of the open pit slope under the influence of various factors was studied. The analysis was conducted based on data collected from the Golgohar iron ore mine in Sirjan. To build the numerical model, first, the geomechanical and hydrogeological parameters of the mine were determined using laboratory and field tests. Then, numerical models of slope stability were built based on the finite difference method using hydromechanical coupling analysis. The real characteristics in these models include lithology types, variations in geomechanical properties, groundwater level, and real slope geometry. Numerical models were built based on three different conditions, including a model in dry conditions, a model considering the groundwater level, and a model after the drainage process. The results show that the whole slope angle of the mine that has the highest safety factor is 36 degrees. In addition, the groundwater level reduces the safety factor of slope stability compared to dry conditions, and the drainage process can increase the safety factor of the mine wall. In all three conditions, the whole slope angle of 36 degrees has the highest safety factor. Therefore, it is suggested that the whole slope angle be considered to increase the safety factor and reduce the stripping ratio to increase the profitability of the open pit mine.

1. Introduction

Rock slope failure in open pit mines is one of the hazards that causes about 14% of injuries and deaths of workers [1]. This highlights the requirement for an extensive study aimed at reducing such risks. It also suggests the requirement to maintain safety as a top priority for safe and profitable ore production. Optimizing the pit angle can improve slope stability and increase profits by reducing stripping [2]. However, this requires a comprehensive understanding of the geotechnical parameters and dynamics of slope movement [3]. Furthermore, the guidelines published by the Canadian Institute of Mines (CIM) for estimating mineral resources and reserves [4] show that for mineral resources recoverable by open-pit mining methods, mineral predictions should not be based solely on economic constraints but must also consider technical requirements (such as slope angles and groundwater table) [5]. With these interpretations, the selection of the whole slope angle of the mine can help mining engineers estimate the mineral resources and plan production from the mine during the open-pit mining process.

In open-pit mines, slope stability is a major concern, and its failure has negative results on the economy and the safety of personnel and equipment. Therefore, it is essential to calculate the safety factor of the rock slope. Slope stability is controlled by various geological conditions and rock mass properties, which are unique to each mine [6]. The slope stability is generally influenced by some factors such as rock strength, slope geometry, discontinues, and groundwater [7, 8]. As

Corresponding author: mfatehi@yazd.ac.ir (M. Fatehi Marji)

the mines deepen, the problems related to the instability of the mine wall will increase.

Groundwater level affects the rock strength of the slope, which decreases the safety factor of the open-pit mine's slope [9]. Due to the importance of this issue, various researchers have conducted some investigations in this field to evaluate the impact of groundwater on slope stability. In the continuation, some of these researches are discussed.

Sjöberg emphasized the critical role of groundwater, geological structure, pit geometry, and rock mass strength in determining slope stability [10]. Stacey and Swart investigated the effect of two factors, such as blasting and groundwater, on slope stability. The results showed that the stability increased by improving the blasting and dewatering [11]. Hustrulid et al. did a slope stability analysis of mine walls using the finite element method and analyzed the influence of groundwater level on the safety factor of slope stability [12]. Eberhardt analyzed the rock slope stability by considering the geological complexity, in situ stresses, anisotropy, and pore pressure [13]. Jiao et al. studied the influence of groundwater on the stability of slopes in weathered igneous rocks in Hong Kong [14]. Read and Stacey studied slope stability by considering various factors such as slope design, complex geology, discontinuities in the rock mass, groundwater level, and blasting [15]. Zhiguo et al. analyzed the stability of the dike slope in Bdg reservoir under flood seepage [16]. Gao et al. investigated the index system of rock slope safety for open pit mines by using fuzzy evaluation and the analytic hierarchy process [17]. Zhao et al. improved the method of using a random angle to generate a random sliding surface for stability analysis of complex slopes [18]. Predrag et al. investigated the impact of weathering on slope stability in soft rock mass [19]. Rabie studied the slope and compared traditional and finite element methods in slopes that are under heavy rainfall [20]. Shao et al. coupled a dual-permeability model with a soil mechanics model for landslide stability evaluation on a hill slope scale by using the COMSOL Multiphysics software [21]. Ahmadi-Adli et al. showed the prediction of seepage and slope stability in a flume test and an experimental field case [22]. Santoso et al. [23] investigated the impacts of groundwater level variation on slope stability in open-pit coal mines. The results found that higher groundwater levels reduce the strength of the slope and decrease the slope stability. Simataa performed the slope stability in an open pit mine and analyzed the groundwater's effect on the slope stability by considering the real geological conditions [24]. Devy and Hutahayan studied the effect of groundwater on slope stability in open-pit mines. The results emphasized the effect of water flow on the reduction of safety factors. Setyananda et al. analyzed the influence of groundwater level on slope stability at Highwall, South Kalimantan, the results showed that the reduction of water level caused to increase in the safety factor [25]. In addition, Zhao et al. improved the method of using a random angle to generate a random sliding surface for stability analysis of complex slopes [26]. Altuntov and Erkayaoglu investigated a new approach to optimize the ultimate geometry of open pit mines with variable whole slope angles [27]. Salu and Bima analyzed the impact of open-pit mining expansion on slope stability. The results showed that the slope geometry and ensuring safety affect the safety factor [28].

Previous studies showed that the slope stability analysis of the pit wall is very complicated, especially when considering the effects of the groundwater table, the whole slope angle, and lithology changes.

Therefore, in this study, the impacts of lithology, groundwater level, and whole slope angle on the slope stability analysis will be investigated. The purpose is to develop the hydromechanical model, estimate the hydrogeological parameters, investigate the effect of drainage, and finally provide the optimal slope angle for this mine. The numerical model of the pit wall was performed based on the finite difference method using the hydromechanical analysis. Real conditions, such as different lithologies, variability in rock properties, groundwater table, and real slope geometry, have been considered. The numerical models were done under three conditions, including dry conditions, considering the groundwater table, and the after-drainage process. The results indicate that the optimized whole slope angle is 36, which has the highest safety factor. The groundwater table can decrease the safety factor of the slope stability compared to the dry conditions, and the drainage process can increase the safety factor. It is advised to apply this whole slope angle to increase the safety factor and decrease the stripping ratio to increase economic profitability.

2. Case study: Golgoahr mine

2.1. General geological setting

The Golgohar iron deposit is located 55 km southwest of Sirjan in the Sanandaj-Sirjan zone (Figure 1). This zone extends from the southwest of central Iran to the northeast of Zagros' main thrust. This zone is approximately 1500 km long. The iron deposit in this zone is located at an altitude of 1740 m and annual rainfall of approximately 120 to 130 mm. The total estimated resource is about 1135 Mt, categorized as one of the main Iranian iron deposits. The rock mass consists of quartzite, sandstone, schists, gabbro, shale, and amphibolite [29].

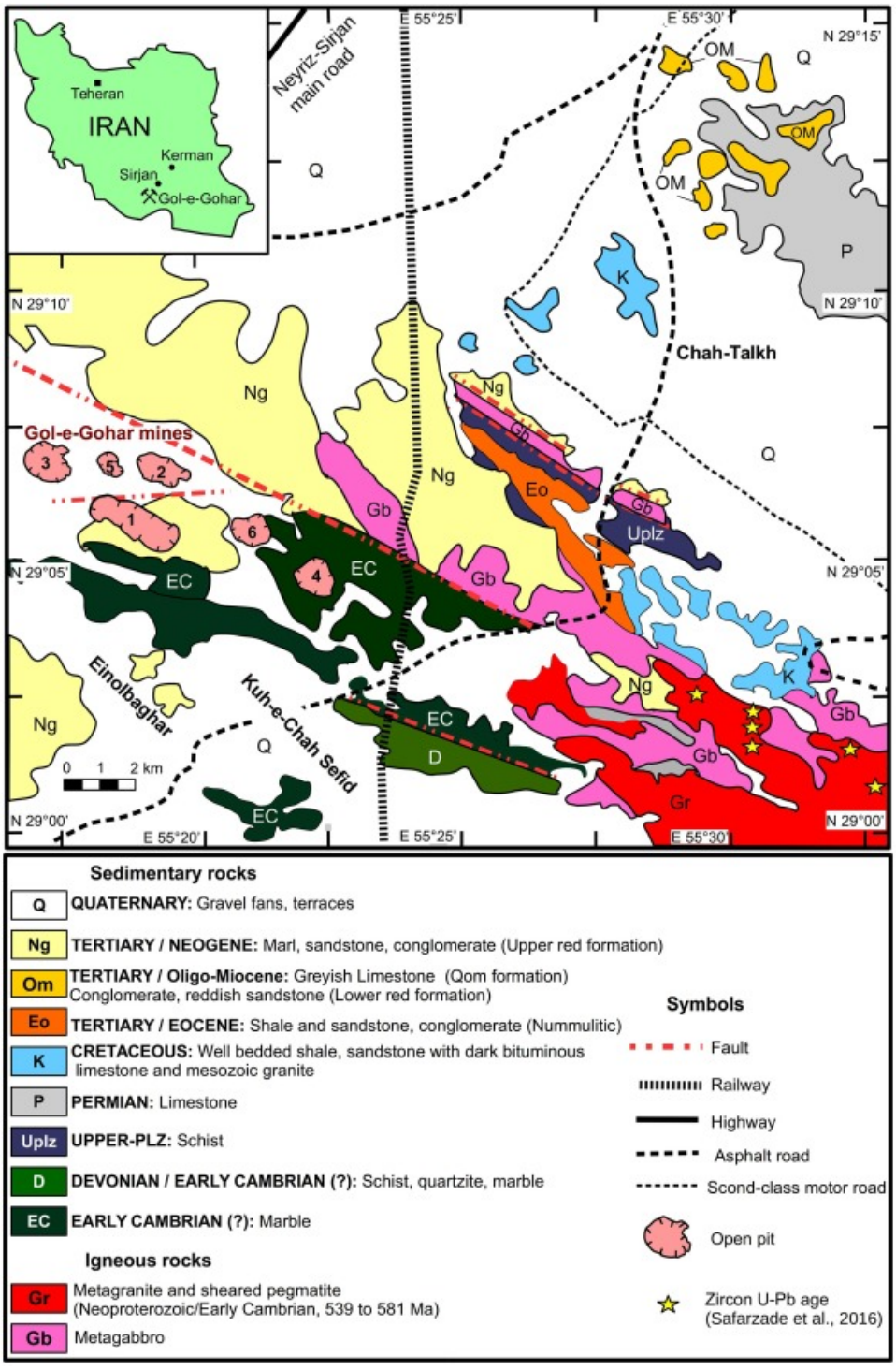

Figure 1. Geological map of the Golgohar iron deposit, Iran [29]

2.2. Discontinuity data collection

Discontinuities were collected by manual mapping on the slope face of different benches in the Golghar mine. A total of two hundred and eighty-four discontinuities have been mapped. The major joint sets were defined by projecting and clustering discontinuity orientations on a stereonet. By using the pole point density method in the Dips software, the dip and dip direction of the joints were obtained. The results showed that there are 4 joint sets with the characteristics stated in Table 1.

2.3. Geomechanical characteristics of rock

The samples were extracted and transported to the rock mechanics lab to assess the geomechanical characteristics of the rock mass. The uniaxial and triaxial tests were done separately for each lithology to measure the quantities of Young's modulus, Poisson ratio, cohesion, and angle of internal friction of intact rock. The information and data obtained from surface surveys of boreholes and laboratory results for existing geological units in different mine zones have been evaluated. Then, using the RocLab software, the strength parameters of different rocks were calculated. The computed data for the geomechanical properties of rock mass are given in Table 2.

Table 1. The joint sets in the Golgohar mine

ID	Joint sets	Dip	Dip direction
G1	J1	68	112
G2	J2	49	23
G3	J3	72	291
G4	J4	46	195

Table 2. Geomechanical properties of rock mass

Lithology	Young modulus [GPa]	Poisson ratio	Cohesion [MPa]	Friction
Alluvium	0.355	0.3	0.23	19
Chlorite schist	1.330	0.22	0.32	25
Mica schist	0.474	0.24	0.24	18
Gneiss	2.234	0.23	0.6	31
Quartz schist	1.326	0.2	0.47	33
Magnetite	4.620	0.18	1.123	38

2.4. Hydrogeological characteristics of rock

There were many limitations to obtaining hydrogeological characteristics; thus, the estimation of these parameters was done indirectly and based on experimental relationships. The following step states the estimation of each parameter and the relationships used.

Špago and Jovanovski [30] stated that estimating the porosity of the rock mass is very complicated. In jointed rocks, by calculating the rock quality index parameter RQD, it is possible to obtain the porosity value by developing empirical relationships between the effective porosity and the rock quality index. Empirical relationships are presented for this purpose, which can be used to estimate porosity.

$$\phi = -0.1583\ RQD + 16.126 \quad (1)$$

And

$$\phi = 19.763\ e^{-0.0243\ RQD} \quad (2)$$

where ϕ is the effective porosity [%] and RQD is the rock quality index [%].

Several relationships have been provided to estimate hydraulic conductivity, some of which are based on the relationship between the rock quality index RQD and hydraulic conductivity K, as stated below:

- **Qureshi et al. [31]**

$$K = 0.01382 - 0.003\ \ln RQD \quad (3)$$

- **El-Naqa [32]**

$$K = 177.45 \exp(-0.0361\ RQD) \quad (4)$$

- **El-Naqa [32, 33]**

$$K = 890.9 \exp(-0.0559\ RQD) \quad (5)$$

- **Jiang et al. [34]**

$$K = 0.4892 \exp(-0.0543\ RQD) \quad (6)$$

where K hydraulic conductivity $[cm/s]$, RQD quality index of rock [%].

In this research, due to the limitations of the measurement test, only three measurement tests were done to compute the value of porosity and hydraulic conductivity of the rock mass. To make a numerical model, much data is required. Therefore, the other data are estimated using empirical

equations. The estimated results are compared with the measured data, as shown in Figure 2, in order to select the right equations for estimating the porosity and hydraulic conductivity.

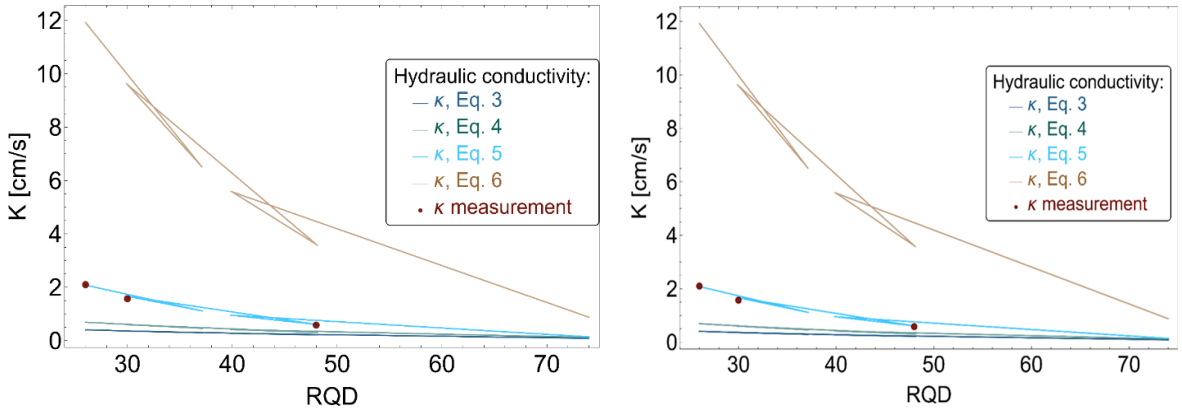

Figure 2. Comparison of estimated and measured data of a) porosity; b) hydraulic conductivity vs RQD

Based on the results, Equation (1) was chosen to estimate the porosity, and Equation (5) was selected to estimate the hydraulic conductivity. Moreover, the relationship between hydraulic conductivity and permeability k is expressed as the following relationship [35]:

$$k = \frac{K\,\mu}{\rho\,g} \tag{7}$$

where ρ is fluid density $[kg/m^3]$, μ is dynamic viscosity $[kg/m\,s]$, g is gravitational acceleration $[m/s^2]$, K is hydraulic conductivity [m/s] and k is permeability $[m^2]$. The computed data for the hydrogeological characteristics of the rock mass are given in Table 3.

Table 3. Hydrogeological characteristics of rock mass

Lithology	RQD	Porosity	Permeability $[m^2]$
Alluvium	26	0.12	$4.06 * 10^{-10}$
Chlorite schist	37	0.1	$2.99 * 10^{-9}$
Mica schist	30	0.11	$3.62 * 10^{-10}$
Gneiss	48	0.09	$3.21 * 10^{-10}$
Quartz schist	40	0.1	$2.75 * 10^{-10}$
Magnetite	74	0.04	$9.08 * 10^{-11}$

3. Theoretical and Mathematical Aspects

The governing equations for hydromechanical coupling are presented based on the mass and momentum equations.

3.1. Mass balance

For single-phase fluid flow in rock mass, the mass balance is as follows [36]:

$$\frac{\partial(\rho_w \phi)}{\partial t} + \nabla \cdot (\rho_w V) = Q - \rho_w \alpha \frac{\partial \varepsilon_v}{\partial t} \tag{8}$$

where ρ_w is the water density, ϕ is the porosity, t is the time, V is the velocity of the mass flow, Q is the source term, ε_v is the volumetric strain of the porous material, and α is the Biot's coefficient. The equation of motion is expressed using Darcy's law as [37, 38]:

$$V = -\frac{k}{\mu_w}(\nabla p + \rho_w g) \tag{9}$$

where k is the permeability and μ_w is the dynamic viscosity of water.

3.2. Momentum balance

Based on the conservation of linear momentum, the equilibrium equation for the rock mass is obtained as [39, 40]:

$$\nabla \cdot (\boldsymbol{\sigma}' - \alpha p I) + \rho g = 0 \tag{10}$$

The constitutive relationship of rock skeleton is [41, 42]:

$$\boldsymbol{\sigma}' = D\boldsymbol{\varepsilon} \tag{11}$$

where $\boldsymbol{\sigma}'$ is the effective stress tensor, $\boldsymbol{\varepsilon}$ is the strain tensor, p is the pore pressure, I is the identity tensor, and ρ is the density, $\rho = (1-\phi)\rho_s + \phi\rho_w$ in which ρ_s is the solid density and ρ_w is water density.

The hydromechanical coupling can be expressed using the combination of Equation (8) and Equation (10). The mentioned equations are the strong form, and to discretize the equations, a numerical scheme is required for the hydromechanical coupling.

3.3. Boundaries and initial conditions

Defining the volume as Ω and the region boundary as Γ, which includes the Neumann and Dirichlet boundaries of the medium. Specific definition: Γ_u is the displacement boundary, Γ_σ is the stress boundary, Γ_p is the pore water pressure boundary, and Γ_q is the flow boundary [41]. The boundary conditions are as follows:

$$\begin{aligned} &u = \bar{u}, \text{ on } \Gamma_u \\ &\text{Given displacement} \\ &\boldsymbol{\sigma}^t \cdot n = \bar{\sigma}, \text{ on } \Gamma_\sigma \\ &\text{Given stress} \end{aligned} \tag{12}$$

And

$$\begin{aligned} &p = \bar{p}, \text{ on } \Gamma_p \\ &\text{Given pore water pressure} \\ &\boldsymbol{q} \cdot n = \bar{q}, \text{ on } \Gamma_q \\ &\text{Given flow} \end{aligned} \tag{13}$$

3.4. Numerical methods

The hydromechanical coupling can be solved using numerical modeling. Generally, there are two main types of numerical models, continuous and discontinuous. The selection of the most adequate numerical approach to simulate the behavior of rock slope will depend on the overall behavior of the rock mass under operation which could be either continuous, homogeneous, and isotropic or discontinuous, inhomogeneous, and anisotropic [43]. Figure 3 summarizes the cases when either continuous or discontinuous numerical modeling is used in rock engineering design. Generally, continuous methods are used either when the rock material is completely intact and has no defects, when there are just a few main planes of weakness (fractures, joints, and discontinuities), or when the rock mass is so highly fractured that its behavior can be assumed equivalent to continuous. Discontinuous modeling is usually used when there are a few main discontinuities that could cause instability or when the failure in the system is mainly governed by the orientation, persistence, size, and strength of the discontinuities.

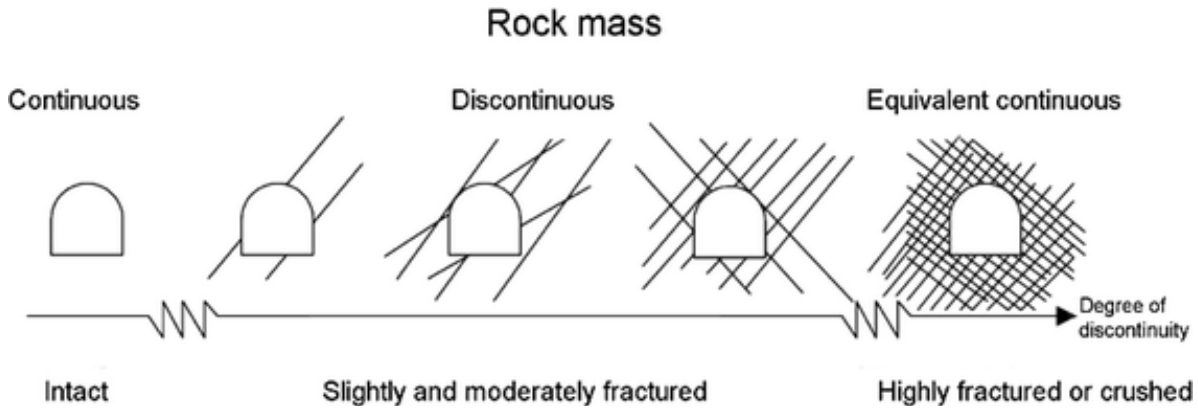

Figure 3. Continuous and discontinuous rock mass behaviors [44]

A rock mass with lots of discontinuities is generally considered a discontinuous system, and discontinuous methods are applied for numerical modeling. However, in large-scale modeling, the presence of discontinuities always increases the volume of calculations, and sometimes the problem is unsolvable. On the other hand, performing a continuum model with laboratory results generally provides unrealistic results. Therefore, in this study, to analyze the structural condition of the region within a mine, a survey of the joints is performed. The results show that four joint sets in the area. Table 1 presents the statistical results of the joint sets in the study area. To characterize the study environment, the Palmström criterion was used in the numerical analysis [45]. Based on the

Palmström criterion, the continuity factor can be computed from Equation (14).

$$CF = \frac{H}{D} \quad (14)$$

where CF is the continuity factor, H is the slope height, and D is the average joint spacing. If the CF value is between 0.01 and 0.2, the environment is discontinuous. On the other hand, for values greater than 100, the environment is considered to be highly jointed and can be modeled continuously. According to the Palmström criterion, by considering the slope height of 260 and the average joint spacing of 0.8, the studied area is placed within the range of fragmented and complex rock structure. The provided information suggests a continuous behavior, and finite difference numerical modeling can be implied for the Golgohar mine.

As stated in this study, the influence of lithology, groundwater, and the whole slope angle on the slope stability is numerically analyzed. The slope stability is analyzed using hydromechanical coupling and by considering different lithologies, groundwater levels, and whole slope angles. The finite difference scheme is applied to discretize the strong form of Equation (8) and Equation (10) to analyze the slope stability.

3.5. Hydro-mechanical coupling strategy in numerical modeling

To express the hydro-mechanical coupling in numerical modeling of the mine slope stability, a specific strategy must be used depending on the numerical method and the type of software selected. In the rest of this paper, it will be stated that in this study, the finite difference method and the FLAC software will be used. Therefore, in this section, the coupling strategy in the FLAC software is expressed. Hydro-mechanical coupling strategy in FLAC was implemented based on the governing equations (Eqs. 8-11) through:

1. **Direct pore-pressure coupling**:
   - Pore pressure (p) is generated from mechanical strains via the $\partial\varepsilon_v/\partial t$ term in Equation 8
   - Effective stress (σ') is updated using Equation 10
2. **Seepage modeling approach**:
   - **Quasi-static transient flow**: Equation 9 (Darcy's law) is solved implicitly at each mechanical step
   - Boundary conditions strictly follow Eqs. 12-13:
     - Prescribed p on vertical boundaries (Γ_p) for dewatering
     - Zero-flux base (Γ_q)
     - Roller constraints (Γ_u)
3. **FISH-enabled automation**:
   - Lithology-specific properties assigned to zones
   - Dynamic boundary updates during dewatering
   - Transient coupling loop (Figure 3) resolved through iterative stress-flow updates

The workflow ensures two-way coupling where mechanical deformations alter pore pressures, which in turn modify effective stresses and failure behavior.

The hydraulic boundary conditions applied in the FLAC model (Figure 10 and Figure 14) were implemented based on the Mathematica-generated geometry. The lateral boundaries are defined by pore pressure along vertical boundaries to represent regional aquifer influence. Also, the water table elevation is dynamically adjustable to simulate dewatering scenarios.

4. Results and Discussions

To analyze the slope stability, hydromechanical coupling is used, which complicates the problem when solving it numerically. The commonly used numerical methods for hydromechanical coupling are Finite Element Method (FEM), Boundary Element Method (BEM), Finite Difference Method (FDM), etc [46]. The finite difference method is a numerical scheme for solving differential equations with given initial and boundary value conditions. In this study, the finite difference method is applied to analyze the slope stability.

4.1. Slope stability analysis

Based on geomechanical study and rock classification systems such as RMR and GSI, the Golgohar Sirjan mine was divided into 8 geomechanical zones as shown in Figure 4. The observations in the mine showed that the A-A' section is mostly affected by groundwater level. Therefore, the analysis of the slope stability of the final wall of the mine at the A-A' section is done to determine the effect of the groundwater level on the safety factor of the mine.

It is important to note that before proceeding with the assessment of the impact of groundwater level on the mine slope stability through safety

factor, numerical modeling validation should be performed. However, it was not possible to access observational data from the Golgohar mine to validate the numerical modeling. At this stage, it can only be suggested that model calibration be performed in the future.

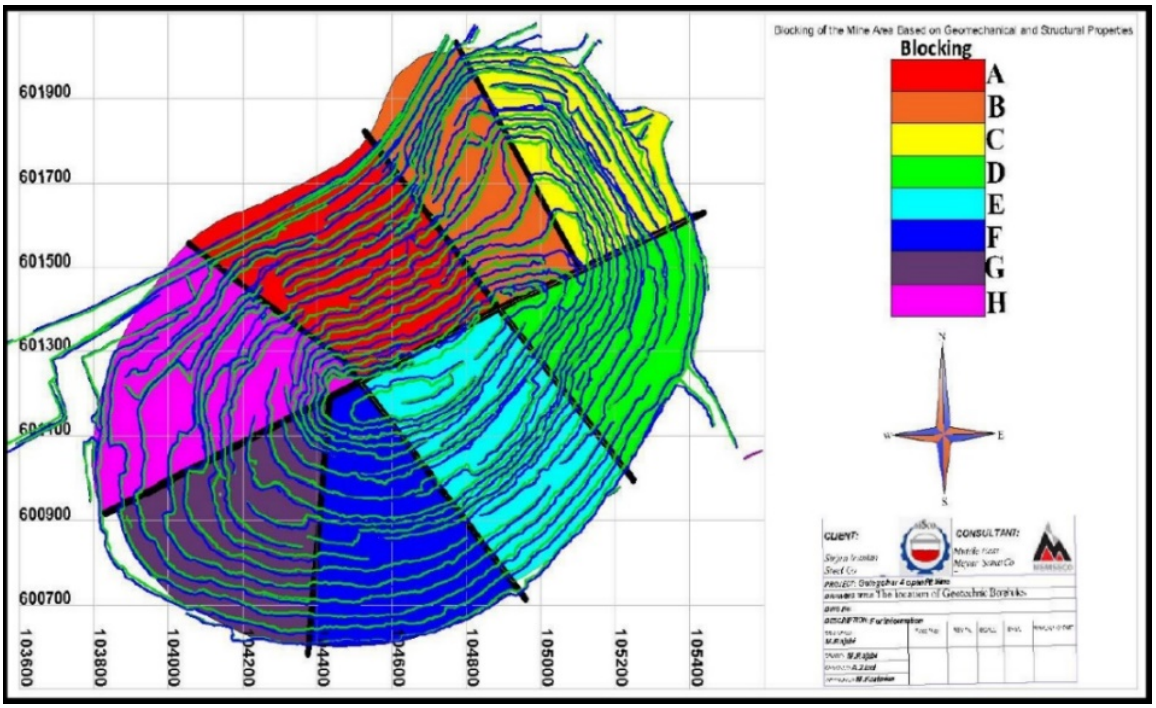

Figure 4. The geomechanical zones of the Golgohar Sirjan mine [47]

The FLAC software is used for numerical modeling of the slope stability while considering hydromechanical behavior. This software is based on the finite difference numerical method (FDM). The corresponding numerical model is done by combining the Fish code language and the graphic environment of this software in the A-A' section. The shape of the geometric model, types of lithology, and slope angle of the mine are shown in Figure 5, and the lithology of the rock mass of the slope is depicted in Figure 6. Geomechanical and hydrogeological characteristics used in this simulation were stated for each lithology in Tables 2 and 3. In this subsection, the numerical modeling of the Golghar mine wall is done in two dry states and considers the hydromechanical behavior.

It should also be noted that in the numerical modeling carried out, an attempt was made to add the anisotropy of the rock mass to the model to some extent so that the model is closer to reality. Regarding lithology, the following rocks were included in the numerical modeling, which are shown in Figure 6b: Alluvium, Quartz schist, Gneiss, Mica schist, Chlorite schist, Magnetite. Regarding structural orientation or heterogeneity, the rock joints of the region were extracted, and after it was proven that the numerical modeling should be continuous. The rock mass data, which includes intact rock, joints, cracks, discontinuities, and faults, etc., were estimated through RockLab. Then, a model similar to the reality of the mine was built. Applying different lithologies to separate rock mass data is, in a way, applying heterogeneity to the aforementioned model.

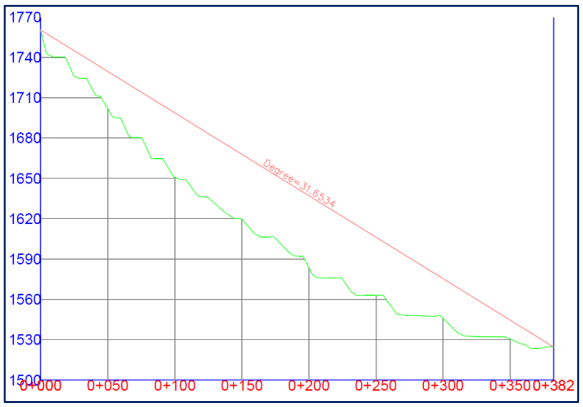

Figure 5. Whole slope angle of the open pit mine in the section A-A'

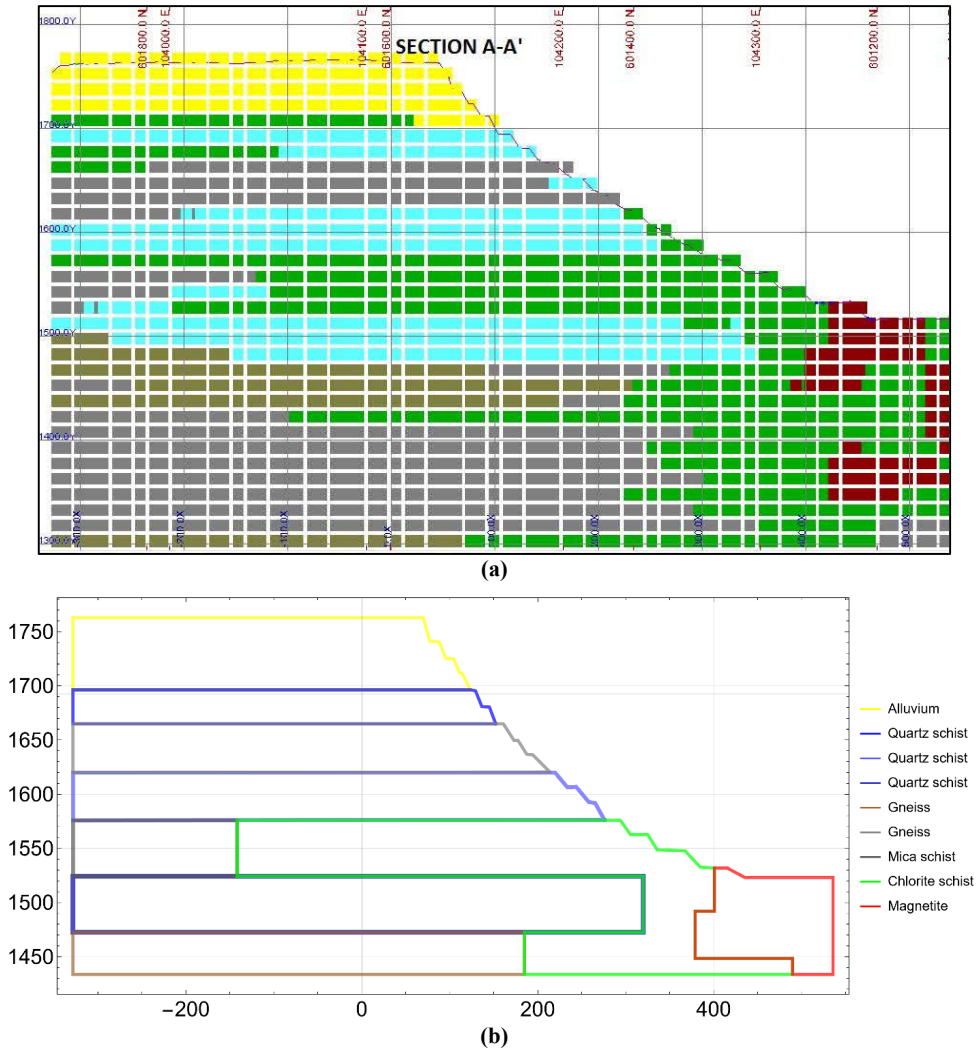

Figure 6. a) Real geometry and lithology of the mine slope, b) Geometry of the mine wall considering its lithologies in section A-A'

In the dry condition, as shown in the field and its numerical geometry in Figure 7, after applying the geomechanical parameters and boundary conditions, the model reaches the initial equilibrium. Then, by modifying displacements, the mentioned model was executed.

The results in the dry state under static analysis are shown in Figure 8 and Figure 9.

The results in Figure 9 illustrate that the safety factor of the pit wall of the mine under dry conditions is equal to 1.45.

For numerical modeling of slope stability by considering the hydromechanical behavior to analyze the effect of groundwater level, it is necessary to include hydrogeological characteristics in the model, which are presented in Table 3. The groundwater level on the left side of the model, compared to the bottom of the model, is equal to 201.5 m and on the right side is equal to 111.5 m (as shown in Figure 10). It means the water height on the left side is 1635.2 m and on the right side is 1545.2 m.

The results of slope stability by considering the hydromechanical modeling are shown in Figures 11 to 13.

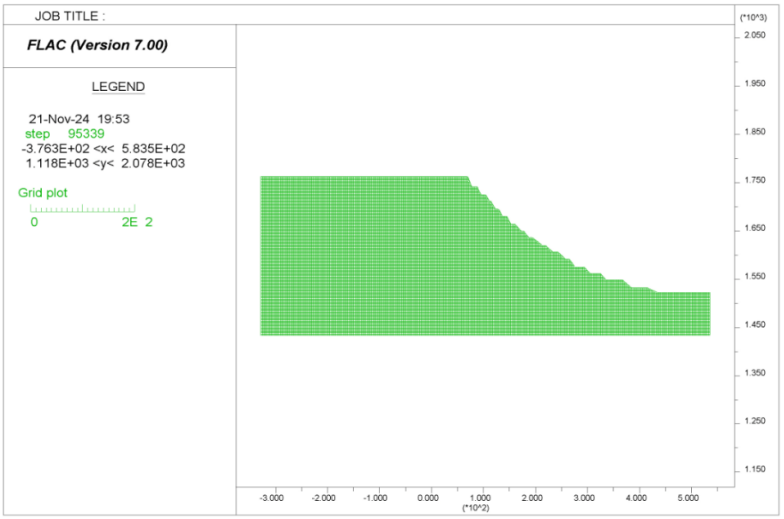

Figure 7. Numerical geometry of the field in dry conditions

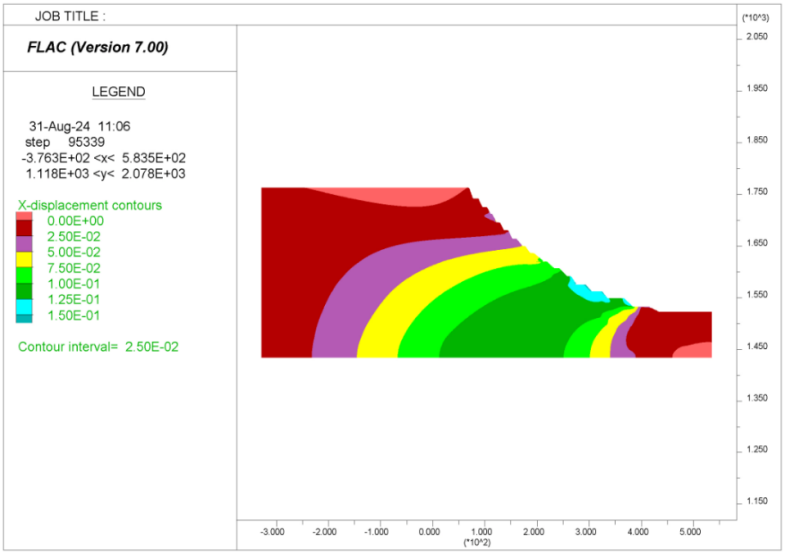

Figure 8. Contour of displacement (m) under dry conditions in X direction

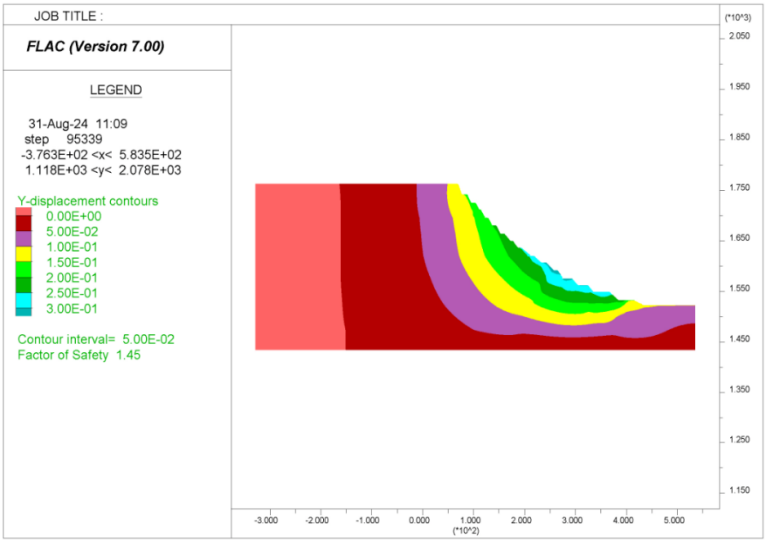

Figure 9. Contour of displacement (m) in Y direction and safety factor under dry conditions

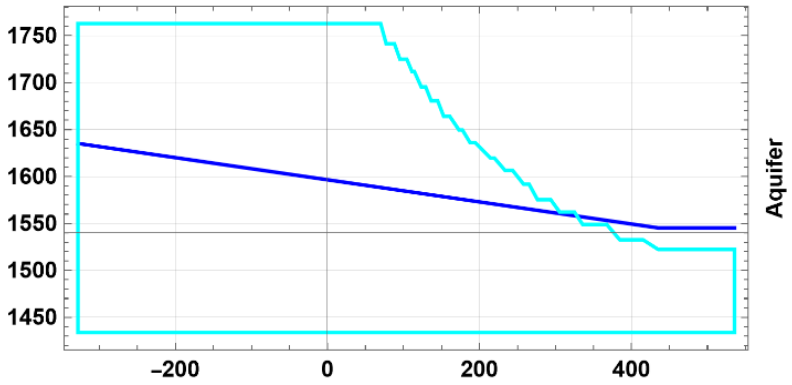

Figure 10. Domain and its geometry by considering the hydromechanical behavior

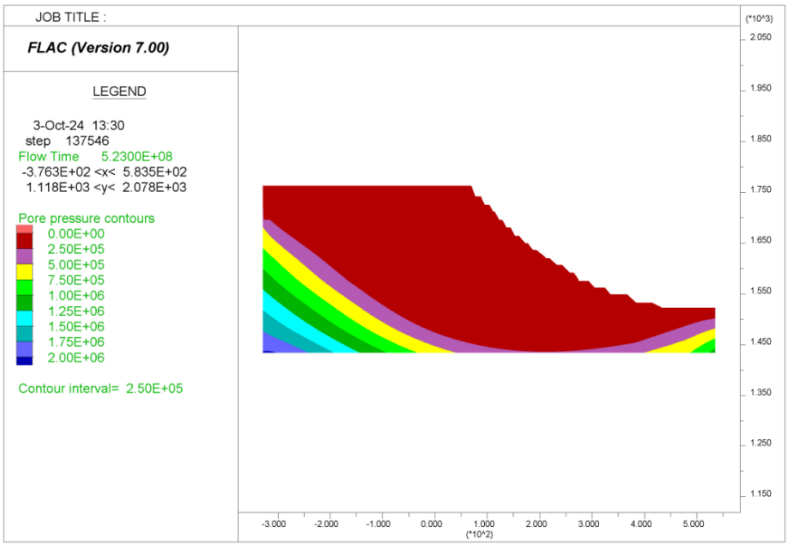

Figure 11. Contour of pore pressure (Pa) by considering the hydromechanical modeling

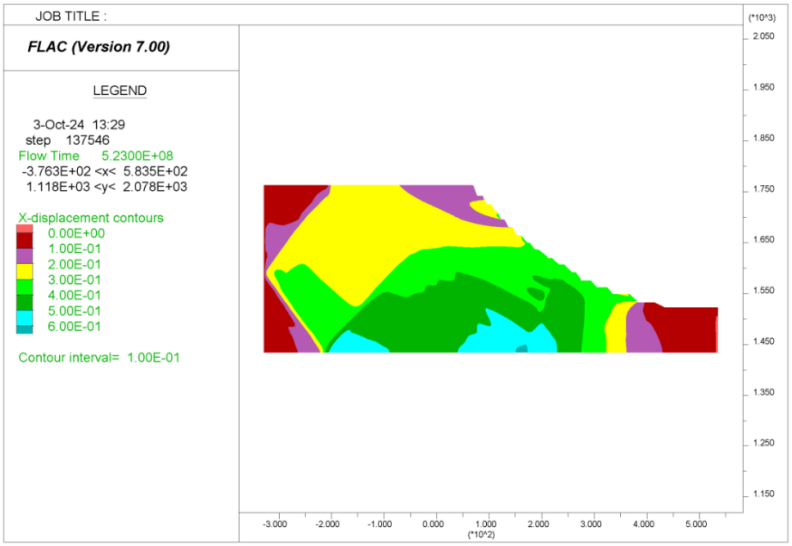

Figure 12. Contour of displacement (m) by considering the hydromechanical modeling in X direction

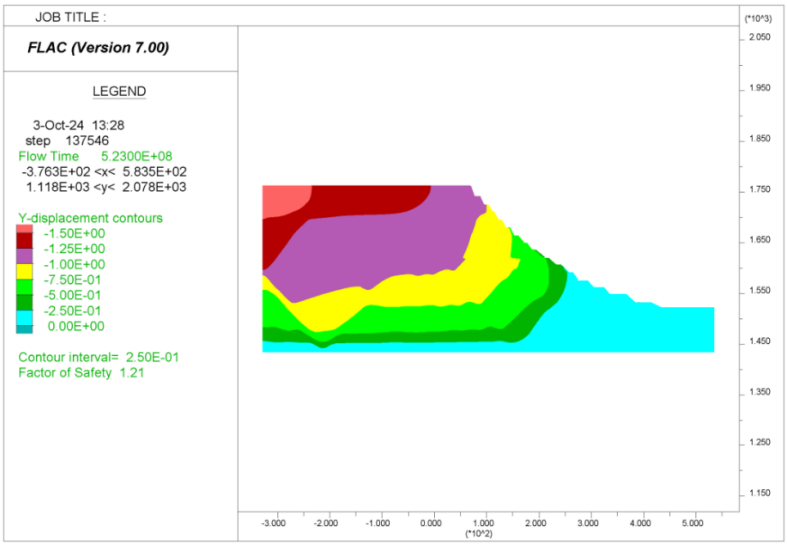

Figure 13. Contour of displacement (m) in Y direction and safety factor by considering the hydromechanical modeling

The results in Figure 13 illustrate that the safety factor of the open-pit wall is 1.21, considering the groundwater level. By comparing the results with the dry condition, the safety factor of the studied wall has decreased by 0.24, which is a significant quantity. This difference shows the necessity of hydromechanical modeling, which helps the model to be closer to the real conditions.

The Y displacement component, as illustrated in Figure 13, has a different sign compared to that of Figure 9. The reason is because of a numerical modeling trick that the user has to do when they want to make a hydromechanical coupling. It means the water table level should be taken as zero, and the other components are modified based on this assumption.

The drainage process was then analyzed using another numerical model developed by the authors. The results show that the mine drainage caused a decrease of about 20 meters in the groundwater level after 3 years compared to the initial state, as shown in Figure 14.

To investigate the slope stability of the mine, the wall under the influence of the drainage process, numerical modeling is done, considering the hydromechanical behavior of the wall. In this model, the groundwater level on the left side of the model compared to the bottom of the model is equal to 181.5 m, and on the right side is equal to 91.5 m. It means the groundwater height on the left side is 1615.2 m and on the right side is 1525.2 m. Moreover, the geomechanical and hydrogeological characteristics in this model are applied based on the data in Tables 2 and 3.

The mentioned modeling is carried out similarly to the initial conditions of the numerical model, and the results of slope stability are presented in Figures 15 to 17.

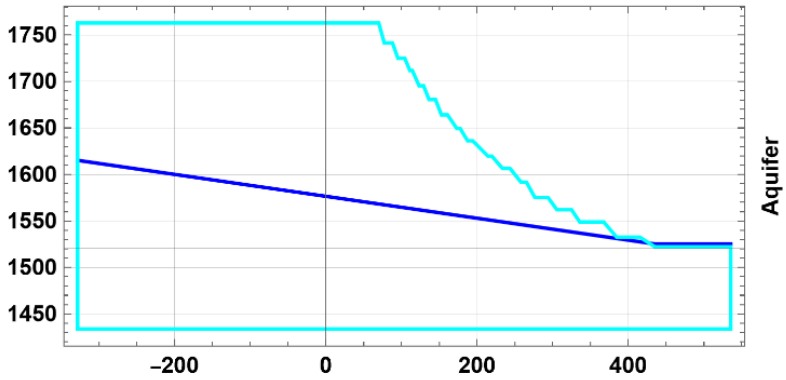

Figure 14. Domain and its geometry by considering the new hydromechanical data

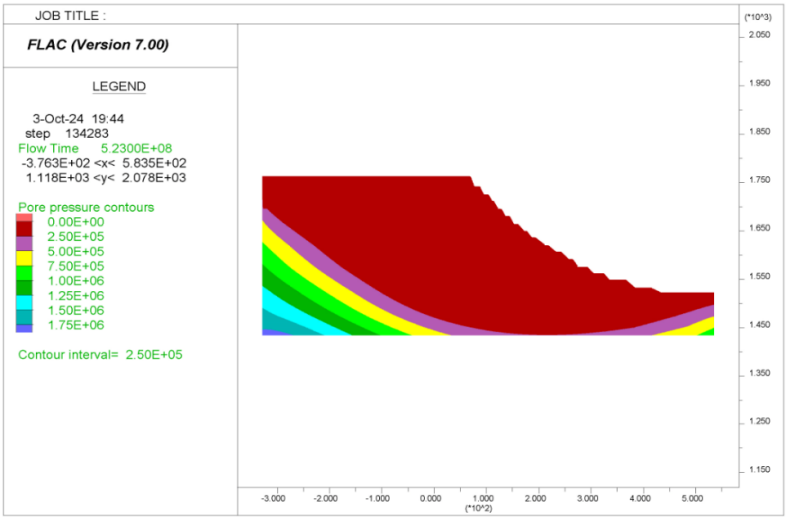

Figure 15. Contour of pore pressure (Pa) by considering the new hydromechanical data

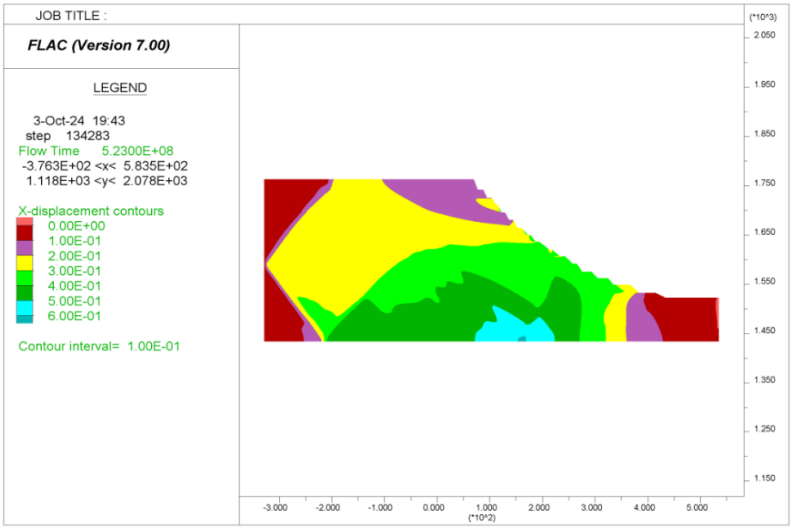

Figure 16. Contour of displacement (m) by considering the new hydromechanical data in the X direction

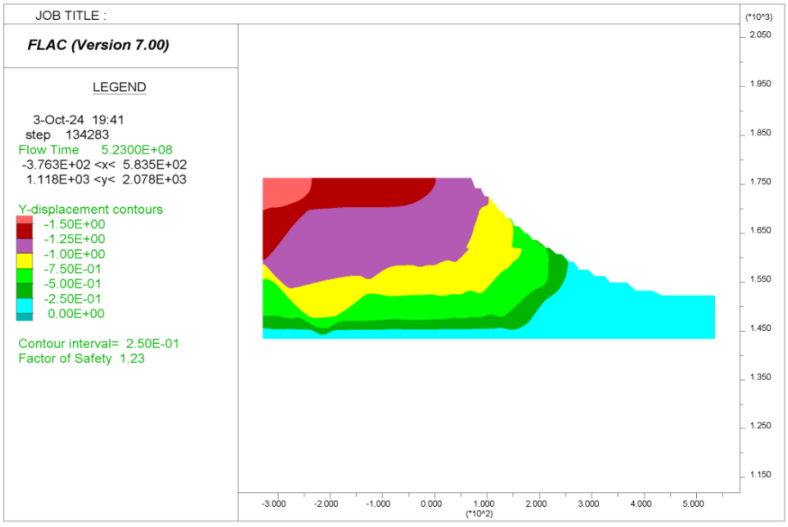

Figure 17. Contour of displacement (m) in the Y direction and safety factor by considering the new hydromechanical data

The results in Figure 17 illustrate that the safety factor of the final wall of the mine by considering the new groundwater level, is 1.23. By comparing the results with the dry condition, the safety factor of the studied wall has decreased by 0.22, which is a large quantity. Furthermore, by comparing the results of this new model with the previous model that considered the groundwater table, the safety factor has increased by 0.02, which is the result of drainage and its importance.

It should be explained that the drainage process can increase the slope stability, but it will not reach a dry condition, because the rock mass is taken as porous media, not the fractured porous media. As you know, the fracture patterns control the water flow in the rock mass and can effectively decrease the safety factor of the slope.

4.2. Slope stability under the influence of various whole slope angles

To investigate the slope stability under the influence of various whole slope angles, numerical modeling is performed. To model and investigate the impact of the whole slope angle of the mine on its stability, different slope angles of the mine wall are selected, which are 31, 33, 35, 36, 38, and 40.

As mentioned in the previous section, these numerical models are carried out based on the real data from the Golgohar mine in Sirjan. The properties of the rock mass and the geometry of the mine slope are the same as those of the mine. Therefore, the numerical results obtained for slope stability cannot be far from reality.

The numerical models are done under three conditions, including the model under dry conditions, the model considering the groundwater table, and the model after the drainage process. The results of the modeling under dry conditions showed that the appropriate range for selecting the optimal mine slope is the range of 31 to 36 degrees because it has the highest safety factor. The results related to different whole slope angles of the wall under dry conditions are presented in Figure 18 and Table 4.

After that, the results of the modeling by considering the first groundwater table illustrated that the suitable range for selecting the optimal mine slope is the range of 35 to 38 degrees, which has the highest safety factor. The results related to different whole slope angles of the wall using the first groundwater table are shown in Figure 19 and Table 5.

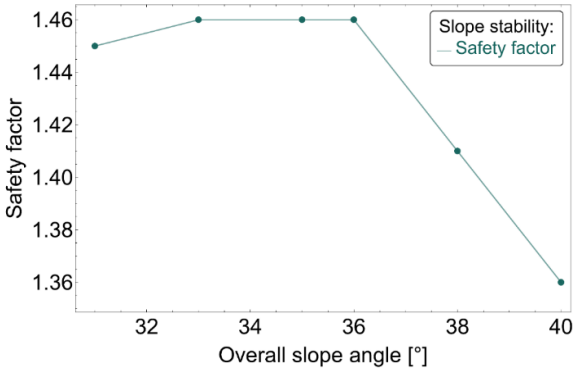

Figure 18. Different whole slope angles versus their safety factors under dry conditions

Table 4. The different whole slope angles versus their safety factors under dry conditions

Whole slope angle	Safety factor
31	1.45
33	1.46
35	1.46
36	1.46
38	1.41
40	1.36

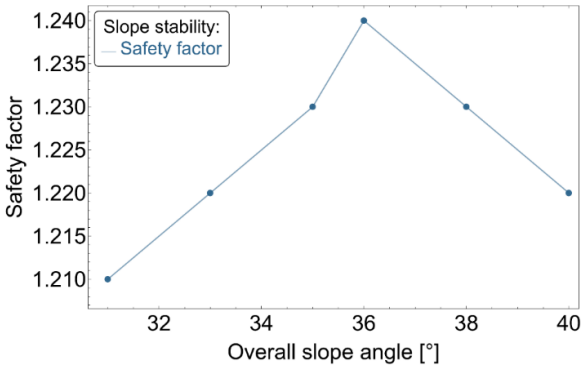

Figure 19. Different whole slope angles versus their safety factors by considering the first groundwater table

Table 5. The different whole slope angles versus their safety factors by considering the first groundwater table

Whole slope angle	Safety factor
31	1.21
33	1.22
35	1.23
36	1.24
38	1.23
40	1.22

Next, the results of the model by considering the second groundwater table showed that the suitable range for choosing the optimal mine slope is the range of 35 to 38 degrees, which has the highest safety factor. The results related to different whole slope angles of the wall by considering the second groundwater table are indicated in Figure 20 and Table 6.

Table 6. The different whole slope angles versus their safety factors by considering the second groundwater table

Whole slope angle	Safety factor
31	1.23
33	1.24
35	1.24
36	1.25
38	1.24
40	1.23

Finally, the results of the whole slope angles versus safety factor changes for all conditions are presented in Figure 21 and Table 7, which emphasizes that the range of 35 to 38 degrees is the most suitable mine whole slope angle (OSA), which has a high safety factor (SF). It is essential to mention that the slope angle of 31 degrees is similar to the real whole slope angle of the mine, and the numerical results also emphasize that it has appropriate safety. However, a better suggestion for the mine slope angle based on the average quantities of safety factor could be an angle of 36 degrees, which has both a higher safety factor and a lower stripping ratio than the current mine slope angle.

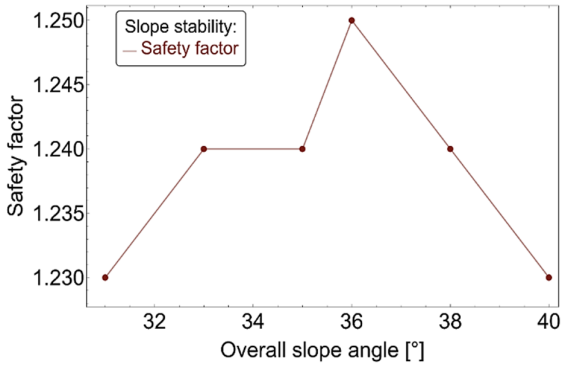

Figure 20. Different whole slope angles versus their safety factors by considering the second groundwater table

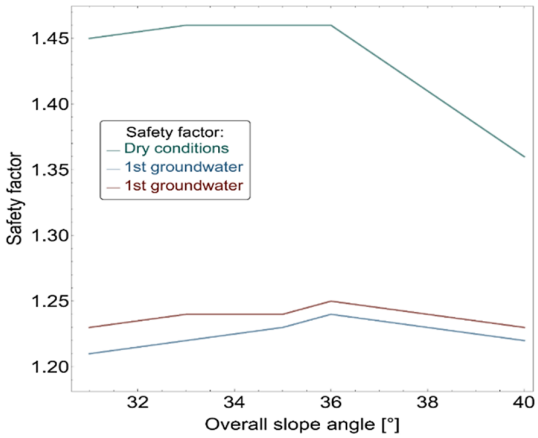

Figure 21. Whole slope angles vs. safety factor changes for all conditions stated

Table 7. The Whole slope angles vs. safety factor changes for all conditions stated

	SF			
OSA	Dry conditions	1st groundwater	2nd groundwater	Average
31	1.45	1.21	1.23	1.296
33	1.46	1.22	1.24	1.306
35	1.46	1.23	1.24	1.310
36	1.46	1.24	1.25	1.316
38	1.41	1.23	1.24	1.293
40	1.36	1.22	1.23	1.270

4.3. Sensitivity Analysis

Sensitivity analysis helps researchers assess the effect of an unknown variable, assuming that other slope parameters are known. In this study, sensitivity analysis was performed for the second groundwater state on three different parameters: Young's modulus, friction angle, and permeability. The choice of each of these parameters is because Young's modulus represents elastic behavior, the friction angle represents plastic behavior, and the permeability represents fluid flow behavior. The sensitivity analysis is done for the 36° optimal slope. The results quantify how ±20% variations in key parameters affect slope safety factors (SF), with all other properties held constant. This sensitivity analysis is reported in Table 8.

Table 8. Sensitivity analysis of slope stability on three parameters: young modulus, the friction angle, and the permeability

Base SF	E variation		ϕ variation		k variation	
SF (E)	SF (0.8 E)	SF (1.2 E)	SF (0.8 ϕ)	SF (1.2 ϕ)	SF (0.5 k)	SF (2 k)
1.25	1.25	1.25	1.04	1.43	1.23	1.26

The results in Table 8 showed that the effect of each parameter on the safety factor is different. Young modulus (E) variations show zero influence on safety factor (SF=1.25 unchanged), confirming that elastic properties affect deformations but not shear failure mechanisms. Friction angle (ϕ) changes dominate stability, with -20% reduction causing 16.8% SF decrease (SF=1.04) and +20% increase yielding 14.4% SF gain (SF=1.43). Permeability (k) adjustments have marginal effects due to effective drainage: halving permeability reduces SF by only 1.6% (SF=1.23), while doubling it increases SF by 0.8% (SF=1.26).

The results demonstrate that while friction angle is the primary control on slope stability (±15% SF variability), permeability plays a secondary role (<2% SF change) in drained conditions, and Young's modulus is irrelevant for safety calculations.

5. Conclusions

In this paper, the aim was to assess numerically the effect of the groundwater and the whole slope angle on the slope stability of the wall in the open pit mine. Some roles, such as groundwater, geological structure, slope geometry, and rock mass strength, were considered to numerically analyze the slope stability. The input data for geomechanical and hydrogeological studies applied to the numerical models were obtained, respectively, using experimental tests and experimental equations. It should be noted that due to the limitation of experimental tests for measuring porosity and permeability of the rock mass, the remaining data are estimated using empirical equations that are expressed in the manuscript. Based on the numerical results, the main conclusions are drawn as follows:

- The slope stability under dry conditions with the whole slope angle of 31 showed the safety factor of the final mine wall was 1.45, which results emphasize that numerical modeling can represent the real conditions.
- The slope stability by considering the groundwater table with the whole slope angle of 31 indicated the safety factor of the pit wall was 1.21. By comparing the hydromechanical model and the model under dry conditions, the safety factor of the wall decreased by 0.24, which was a significant quantity.
- The slope stability by considering the new groundwater level showed the safety factor of the final mine wall with the whole slope angle 31 was 1.23, which results emphasize that the safety factor increased by 0.02 compared to the 1st groundwater, which was the result of drainage and its importance.
- The results of slope stability under dry conditions emphasized that the range of 31 to 36 degrees is a suitable mine whole slope angle.
- The slope stability results, considering the groundwater level, emphasized that the range of 35 to 38 degrees is a suitable whole slope angle for the mine.
- A better suggestion for the mine slope angle based on the average quantities of safety factor could be an angle of 36 degrees, which has both a higher safety factor and a lower stripping ratio than the current mine slope angle. This angle can increase economic profitability.
- The sensitivity analysis was performed for the second groundwater state on three different parameters: Young's modulus, friction angle, and permeability. It was done for the 36° optimal slope. The results showed that the friction angle is the primary control on slope stability (±15% SF variability); also, permeability plays a secondary role (<2% SF change) in drained conditions, and Young's modulus is irrelevant for safety calculations.

References

[1]. Aleotti, P., & Chowdhury, R. (1999). Landslide Hazard Assessment: Summary Review and New Perspectives. *Bulletin of Engineering Geology and the Environment, 58*, 21-44.

[2]. Read, J., & Stacey, P. (2009). Guidelines for open-pit slope design. *CSIRO Publishing, Collingwood, VIC, Australia*.

[3]. Quansah, E. A., Anani, A., & Adewuyi, S. (2024). Optimizing Overall Slope Angle and Net Present Value (NPV) Through the Utilization of Ground-Based Pit Wall Monitoring Data. *In the 58th U.S. Rock Mechanics/Geomechanics Symposium. 58th U.S. Rock Mechanics/Geomechanics Symposium. ARMA*.

[4]. CIM. (2019). CIM Estimation of Mineral Resources and Mineral Reserves Best Practice Guidelines. Retrieved from https://www.bcsc.bc.ca/-/media/PWS/Resources/For_Companies/Mining/CIM-Best-Practices-Guidelines-November- 29-2019.pdf.

[5]. Altuntov, F. K., & Erkayaoğlu, M. (2021). A New Approach to Optimize Ultimate Geometry of Open Pit Mines with Variable Overall Slope Angles. In Natural Resources Research. *Springer Science and Business Media LLC, 30*(6), 4047–4062.

[6]. Kumar, V., & Parkash, V. (2015). A model study of slope stability in mines situated in South India. *Adv. Appl. Sci. Res. 6*, 82-90.

[7]. Liu, W., Sheng, G., Kang, X., Yang, M., Li, D., & Wu, S. (2024). Slope Stability Analysis of Open-Pit Mine Considering Weathering Effects. *Applied Sciences, 14*(18), 8449.

[8]. Bezie, G., Chala, E.T., Jilo, N.Z. et al. (2024). Rock slope stability analysis of a limestone quarry in a case study of a National Cement Factory in Eastern Ethiopia. *Sci Rep 14*, 18541.

[9]. Jelani, J., Adnan, N., Husen, H., Mohd Daud, M.N., & Sojipto, S. (2020). The effects of ground water level fluctuation on slope stability. *Zulfaqar Journal of Defence Science, Engineering & Technology, 3*(1).

[10]. Sjöberg, J. (1996). Large scale slope stability in open pit mining: a review.

[11]. Stacey, T. R., & Swart, A. H. (2001). Booklet Practical Rock Engineering Practice for Shallow and Opencast Mines, Johannesburg. The Safety in Mines Research Advisory Committee (SIMRAC).

[12]. Hustrulid, W.A., Mccarter, M.K., & Zyl, D.J.A. (2001). Slope Stability in Surface Mining.

[13]. Eberhardt, E. (2003). Rock slope stability analysis—utilization of advanced numerical techniques, *Earth Ocean Sci. UBC Vanc*. Canada.

[14]. Jiao, J.J., X.S. Wang, & S. Nandy. (2005). Confined groundwater zone and slope instability in weathered igneous rocks in Hong Kong. *Engineering Geology, 80*(1), 71-92.

[15]. Read, J., & Stacey, P. (2009). Guidelines for Open Pit Slope Design, CSIRO Publishing.

[16]. Niu Zhiguo, et al. (2011). The stability analysis of the dike slope in Bdg reservoir under the seepage of flood. *Procedia Engineering 15*, 5263-5267.

[17]. Yu-kun, G., ZHANG, B.N., Li-ming, L., & Zhian, H. (2011). Research on index system of rock slope safety evaluation for open pit mine. *Procedia Engineering, 26*, 1692-1697.

[18]. Weifeng, Z., Lianheng, Z., & Dongping, D. (2012). Improved Sliding Surface Search Method for Stability Analysis of Complex Slopes. International Conference on Structural Computation and Geotechnical Mechanics.

[19]. Miscevic, P., & Vlastelica, G. (2014). Impact of weathering on slope stability in soft rock mass "*Journal of Rock Mechanics and Geotechnical Engineering, 6*, 240-250.

[20]. Rabie, M. (2014). Comparison study between traditional and finite element methods for slopes under heavy rainfall. *HBRC Journal, 10*, 160-168.

[21]. Shao, W., Bogaard, T.H., & Bakker, M. (2014). How to Use COMSOL Multiphysics for coupled dual-permeability hydrological and slope stability modeling" *Procedia Earth and Planetary Science, 9*, 83-90.

[22]. Ahmadi-Adli, M., Kartal Toker, N., & Huvaj, N. (2014). Prediction of seepage and slope stability in a flume test and an experimental field case. *Procedia Earth and Planetary Science, 9*,189-194.

[23]. Simataa, E. (2019). Investigating slope stability in an open pit mine - a case study of the phyllites western wall at sentinel pit.

[24]. Devy, S. D., & Hutahayan, P. P. (2021). Groundwater Effect on Slope Stability in Open Pit Mining: a Case of West Kutai Regency, East Kalimantan, Indonesia. *In Journal of Geoscience, Engineering, Environment, and Technology, 6*(4), 192-205.

[25]. Setyananda, A., Novi Hartami, P., Maulana, Y., Jamal Tuheteru, E., Korra Herdyanti, M., & Putra, D. (2024). Analysis of the Influence of Groundwater Level on Slope Stability at Highwall PT. X, South Kalimantan. In IOP Conference Series: *Earth and Environmental Science, 1339*(1), 012029. IOP Publishing.

[26]. Weifeng, Z., Lianheng, Z., & Dongping, D. (2012). Improved Sliding Surface Search Method for Stability Analysis of Complex Slopes. *International Conference on Structural Computation and Geotechnical Mechanics*.

[27]. Altuntov, F. K., & Erkayaoğlu, M. (2021). A New Approach to Optimize Ultimate Geometry of Open Pit Mines with Variable Overall Slope Angles. *In Natural Resources Research, 30*(6), 4047–4062. Springer Science and Business Media LLC.

[28]. Salu, S., & Bima, B. (2024). The Impact of Mine Opening Expansion on Slope Stability: A Case Study in North Konawe Southeast Sulawesi Province Indonesia. Journal of Mining and Environment, Online First.

[29]. Alibabaie, N., Esmaeily, D., Peters, S. T. M., Horn, I., Gerdes., A., Nirooamand, S., Jian, W., Mansouri, T., Tudeshki, H., & Lehmann, B. (2020). Evolution of the Kiruna-type Gol-e-Gohar iron ore district, Sanandaj-Sirjan zone, Iran. *In Ore Geology Reviews, 127*, 103787. Elsevier BV.

[30]. Špago, A., & Jovanovski, M. (2019) Applicability of the Geological Strength Index (GSI) classification for carbonate rock mass Primjena "Geological Strength Index" (GSI) klasifikacije na karbonatne stijenske massive. *Conference of Geotechnical chalenges in Karts, Omis, Croatia*.

[31]. Qureshi, M.U., K. M. Khan, N. Bessaih, K. Al-Mawali & K. Al-Sadrani. (2014). An empirical relationship between in-situ permeability and RQD of discontinuous sedimentary rocks. *Electronic Journal of Geotechnical Engineering, 19*, 4781-4790.

[32]. El-Naqa, A. (2001). The hydraulic conductivity of the fractures intersecting Cambrian sandstone rock masses, central Jordan. *Environmental Geology, 40*(8), 973-982.

[33]. Shahbazi, A., Saeidi, A., & Chesnaux, R. (2020). A review of existing methods used to evaluate the hydraulic conductivity of a fractured rock mass. *In Engineering Geology, 265*, 105438.

[34]. Jiang, X. W., L. Wan, X. S. Wang, X. Wu & X. Zhang. (2009). Estimation of rock mass deformation modulus using variations in transmissivity and RQD with depth. *International Journal of Rock Mechanics and Mining Sciences 46*(8), 1370-1377.

[35]. Atangana, A. (2018). Aquifers and Their Properties. In Fractional Operators with Constant and Variable Order with Application to Geo-Hydrology, 1-13.

[36]. Zhao, C., Zhang, Z., & Lei, Q. (2021). Role of hydro-mechanical coupling in excavation-induced damage propagation, fracture deformation and microseismicity evolution in naturally fractured rocks. *In Engineering Geology 289*, 106169. Elsevier BV.

[37]. Sanei, M. (2020). Numerical and experimental study of coupled nonlinear geomechanics and fluid flow applied to reservoir simulation. PhD thesis of State University of Campinas.

[38]. Duran, O., Sanei, M., Devloo, P.R.B. et al. (2020). An enhanced sequential fully implicit scheme for reservoir geomechanics. *Comput Geosci 24*, 1557–1587.

[39]. Sanei, M., Duran, O., Devloo, P.R.B. et al. (2021). Analysis of pore collapse and shear-enhanced compaction in hydrocarbon reservoirs using coupled poro-elastoplasticity and permeability. *Arab J Geosci 14*, 645.

[40]. Sanei, M., Duran, O., Devloo, P.R.B. (2019). Numerical modeling of pore collapse in hydrocarbon reservoirs using a cap plasticity constitutive model. In Proceedings of the 14th International Congress on Rock Mechanics and Rock Engineering, Brazil. ISRM14CONGRESS-2019-377.

[41]. Zhao, Y., Liu, Q., Lin, H., Wang, Y., Tang, W., Liao, J., Li, Y., & Wang, X. (2023). A Review of Hydromechanical Coupling Tests, Theoretical and Numerical Analyses in Rock Materials. *Water, 15*(13), 2309.

[42]. Sanei, M., Duran, O., Devloo, P.R.B. et al. (2022). Evaluation of the impact of strain-dependent permeability on reservoir productivity using iterative coupled reservoir geomechanical modeling. Geomech. Geophys. *Geo-energ. Geo-resour. 8*, 54.

[43]. Hudson, J., & Harrison, J. (2000). Engineering Rock Mechanics: An Introduction to the Principles, 2(2000), 114. London: Elsevier Science Ltd.

[44]. Eldebro C. (2003). Rock mass strength—a review. Technical Report, Lulea˚ University of Technology, Lulea.

[45]. Palmström, A. (1995). Characterizing rock burst and squeezing by the rock mass index. *International conference in design and construction of underground structures. 10*, 10.

[46]. Bobet, A. (2010). Numerical Methods in Geo-Mechanics. *The Arabian Journal for Science and Engineering, 35*, 27-48.

[47]. Geomechanical report of Golgohar Sirjan mine. (2024).

نشریه مهندسی معدن و محیط زیست
نشانی نشریه: www.jme.shahroodut.ac.ir
انجمن مهندسی معدن ایران
دانشگاه صنعتی شاهرود

بررسی اثرات همزمان هندسه، لیتولوژی، زاویه شیب و سطح آب زیرزمینی بر پایداری شیب معادن روباز (مطالعه موردی معدن سنگ آهن گل‌گهر، سیرجان، ایران)

محمد شکاری نژاد[1]، محمد فاتحی مرجی[2*] و منوچهر صانعی[2]

۱. دانشکده مهندسی معدن، دانشگاه آزاد اسلامی، سیرجان، ایران
۲. دانشکده مهندسی معدن و متالورژی، دانشگاه یزد، یزد، ایران

اطلاعات مقاله

تاریخ ارسال: ۲۰۲۵/۰۳/۰۴
تاریخ داوری: ۲۰۲۵/۰۷/۲۷
تاریخ پذیرش: ۲۰۲۵/۰۸/۲۶

DOI: 10.22044/jme.2025.15867.3055

کلمات کلیدی

پایداری شیب دیواره
مدل‌سازی هیدرومکانیکی
زهکشی
زاویه شیب کلی
ضریب ایمنی

چکیده

هندسه شیب دیواره، کیفیت توده سنگ، سطح آب زیرزمینی و ویژگی‌های زمین‌شناسی معدن عمدتاً بر پایداری شیب یک معدن روباز تأثیر می‌گذارند. در این مطالعه، تحلیل پایداری شیب دیواره معدن روباز تحت تأثیر عوامل مختلف مورد بررسی قرار گرفت. این تحلیل بر اساس داده‌های جمع‌آوری‌شده از معدن سنگ آهن گل‌گهر در سیرجان انجام شد. برای ساخت مدل عددی، ابتدا پارامترهای ژئومکانیکی و هیدروژئولوژیکی معدن با استفاده از آزمایش‌های آزمایشگاهی و میدانی تعیین شدند. سپس، مدل‌های عددی پایداری شیب دیواره بر اساس روش تفاضل محدود با استفاده از تحلیل کوپل هیدرومکانیک ساخته شدند. ویژگی‌های واقعی در این مدل‌ها شامل انواع لیتولوژی، تغییرات خواص ژئومکانیکی، سطح آب زیرزمینی و هندسه شیب واقعی دیواره است. مدل‌های عددی بر اساس سه حالت مختلف که شامل یک مدل در شرایط خشک، یک مدل با در نظر گرفتن سطح آب زیرزمینی و یک مدل پس از فرآیند زهکشی، ساخته شدند. نتایج نشان می‌دهد که زاویه شیب دیواره معدن که بالاترین ضریب ایمنی را دارد، ۳۶ درجه است. علاوه بر این، سطح آب زیرزمینی ضریب ایمنی پایداری شیب دیواره را در مقایسه با شرایط خشک کاهش می‌دهد و فرآیند زهکشی می‌تواند ضریب ایمنی دیواره معدن را افزایش دهد. در هر سه حالت، زاویه شیب کلی ۳۶ درجه بیشترین ضریب ایمنی را دارد. بنابراین پیشنهاد می‌شود برای افزایش ضریب ایمنی و کاهش نسبت باطله‌برداری، زاویه شیب کلی در معدن ۳۶ درجه در نظر گرفته شود تا سودآوری معدن روباز افزایش یابد..

نویسنده مسئول مکاتبات: mfatehi@yazd.ac.ir (م. فاتحی مرجی)